Journal of Global Positioning Systems (2003)
Vol. 2, No. 1: 48-55

Regional Ionosphere Mapping with Kriging and Multiquadric Methods

Pawel Wielgosz[1,2], Dorota Grejner-Brzezinska[1], Israel Kashani[1,3]

[1]The Ohio State University, CEEGS, 470 Hitchcock Hall, 2070 Neil Avenue, Columbus, OH 43210-1275
e-mail: Wielgosz.1@osu.edu, tel.: 614-292-0169, fax: 614-292-2957

[2] University of Warmia and Mazury in Olsztyn, Poland

[3]Technion - Israel Institute of Technology

Received: 14 October 2003 / Accepted: 27 November 2003

Abstract. This paper demonstrates the concept and practical examples of instantaneous mapping of regional ionosphere, based on GPS observations from the State of Ohio continuously operating reference stations (CORS) network. Interpolation/prediction techniques, such as kriging (KR) and the Multiquadric Model (MQ), which are suitable for handling multi-scale phenomena and unevenly distributed data, were used to create total electron content (TEC) maps. Their computational efficiency (especially the MQ technique) and the ability to handle undersampled data (especially kriging) are particularly attractive. Presented here are the preliminary results based on GPS observations collected at five Ohio CORS stations (~100 km station separation and 1-second sampling rate). Dual frequency carrier phase and code GPS observations were used. A zero-difference approach was used for absolute TEC recovery. The quality of the ionosphere representation was tested by comparison to the International GPS Service (IGS) Global Ionosphere Maps (GIMs), which were used as a reference.

Key words: GPS, Ionosphere, Kriging, IGS

1 Introduction

Spatial and temporal characteristics of the ionosphere are of primary interest in their own scientific context, but they are also of special interest to communication, surveillance and safety-critical systems, as they affect the skywave signal channel characteristics. According to Stanislawska et al. (2002), the epoch-specific instantaneous maps of ionospheric parameters are of great importance in assessing the radio propagation effects on terrestrial and Earth-space radio communication and navigation, and for aeronomical studies. Instantaneous ionosphere mapping is defined as a technique applying simultaneously measured total electron content (TEC) values at a limited number of locations to generate TEC maps referred to a specific time epoch (Stanislawska et al., 2000). Instantaneous mapping can be applied in near real or real time, and is (theoretically) limited only by the speed of accessing the data from the tracking stations. The time series of the instantaneous TEC maps can be used to derive average monthly maps describing major ionospheric trends as a function of local time, season, and spatial location. In addition, the results of the statistical analysis of a time/space series can support ionosphere forecasting and nowcasting.

With a large number of permanently tracking stations, GPS can deliver large volumes of data suitable for continuous, near or real-time ionosphere monitoring during disturbed and quiet geomagnetic conditions, and offers an attractive alternative to traditional methods (e.g., ionosonde network). Currently, GPS analysis centers provide GIMs (Global Ionosphere Maps) on a daily basis. The widely used GPS-derived GIMs provided by the International GPS Service (IGS) have a spatial resolution of 2.5º and 5.0º in latitude and longitude, respectively, and a 2-hour temporal resolution (Feltens and Jakowski, 2002). Thus, although IGS supports the scientific community with quality GPS products, IGS GIMs cannot reproduce local, short-lasting processes in the ionosphere. In addition, the resolution of these products might not be sufficient to support high quality GPS positioning, especially in the presence of local ionospheric disturbances. The need to produce high-resolution regional ionosphere models, supporting

Some results presented here were reported at ION GNSS 2003, Portland, OR navigation, static positioning and space weather research, is commonly recognized (Komjathy, 1997; Hernandez-Pajares et al., 1999; Gao and Liu, 2002).

Many GPS ionosphere-modeling algorithms are based on spherical harmonics (SH) expansion (Schaer, 1999; Wielgosz et al., 2003), which is not very effective in handling multi-scale phenomena and nonhomogeneous fields, due to their global nature (Li, 1999; Schmidt, 2001). Therefore, alternative methods that are more suitable for the modeling of nonhomogeneous fields, such as the ionosphere, are studied in this paper. Gao and Liu (2002) pointed out that interpolation methods might give comparable or even better results, compared to the mathematical function representation of TEC. Thus, we propose to investigate the suitability of the two estimation/interpolation techniques, kriging (KR) and Multiquadric Model (MQ), for regional ionosphere mapping.

2 Methodology

2.1 Absolute TEC determination

The presented approach uses double frequency GPS phase and code observations collected at the reference station network. Carrier phase observations are used to smooth pseudoranges, as described by Springer (1999). After the smoothing procedure, the pseudoranges are effectively replaced by phase observations with approximated (real-valued) ambiguities. The Differential Code Biases (DCBs) for satellites are provided by IGS (through the Internet) and the DCBs for the receivers are derived from the GPS receivers' calibration performed using the BERNESE software (Hugentobler et al., 2001). The geometry-free linear combination of un-differenced GPS observations is applied in order to derive the instantaneous ionosphere as described below (Eqs. 1, 2 and 3). The undifferenced pseudorange geometry-free linear combination, primarily used to obtain ionospheric information from the GPS observations, is as follows (Schaer, 1999):

$$\tilde{P}_{i,4}^k = \tilde{P}_{i,1}^k - \tilde{P}_{i,2}^k = \xi_4 I_i^k + c(\Delta b^k + \Delta b_i) \quad (1)$$

The ionospheric delay related to the first GPS frequency can be derived from the formula:

$$I_i^k = (\tilde{P}_{i,4}^k - c(\Delta b^k + \Delta b_i)) / \xi_4 \quad (2)$$

where:

$\tilde{P}_{i,4}^k$ - undifferenced pseudorange geometry-free linear combination of smoothed code observations

$\tilde{P}_{i,n}^k$ - carrier-smoothed code observation on frequency n (n=1,2)

I_i^k - ionospheric delay

c - speed of light

Δb^k - DCB for a satellite *k*

Δb_i - DCB for a receiver *i*

ξ_4 - coefficient converting ionospheric delay on P_4 to P_1

The relationship between the absolute TEC and the ionospheric delay is described as follows (Schaer, 1999):

$$I_i^k = \pm \frac{C_x}{2} TEC f_1^{-2} = \xi_{TEC} TEC \quad (3)$$

Where the proportionality factor is:

$$\frac{C_x}{2} = 40.3 \times 10^{16}\ \mathrm{ms^{-2}/TECU},$$

and the ionospheric delay caused by 1 TECU on the first GPS frequency is:

$$\xi_{TEC} = 0.162\ \mathrm{m/TECU}$$

while the first GPS frequency is denoted as f_1.

2.2 Single layer model - SLM

For the TEC representation, a single layer model (SLM) ionosphere approximation was used (Fig. 1). SLM assumes that all the free electrons are contained in a shell of infinitesimal thickness at altitude *H*. A mapping function converting slant TEC to the vertical one is needed, as shown in Eq. 4 (Mannucci et al., 1993):

$$F(z) = [1 - \frac{R\cos(90 - z)}{R + H}]^{-0.5} \quad (4)$$

where:

R - Earth radius
H - SLM height
z - satellite zenith angle

When using the above mapping function *F(z),* one can obtain vertical TEC values at the ionosphere pierce points (IPPs). It can be easily shown that a single GPS receiver can probe the ionosphere in a radius of 960 km assuming 20° elevation cut-off angle and 450 km SLM height (Schaer, 1999; see also IGS IONEX file header).

2.3 Kriging interpolation method

Kriging is an estimation and interpolation method applied in geostatistics, which uses known sample values and a variogram to determine the unknown values at different locations/times. It utilizes the spatial and temporal correlation properties of the underlying phenomenon, and incorporates the measures of the error and uncertainty when determining the estimates (Webster and Oliver, 2001; Stanislawska et al., 1999 and 2002). At each location kriging produces an estimate and a confidence bound on the estimate, i.e., the kriging variance. The uncertainty maps associated with kriging appear to naturally account for insufficient sampling. Blanch (2002) demonstrated that kriging could successfully mitigate the undersampled problem due to sparse data points.

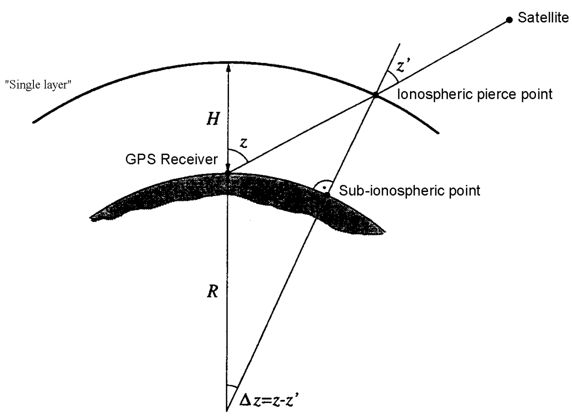

Fig. 1 Single layer model of the ionosphere (Schaer, 1999)

2.4 Multi-quadric model

The alternative to kriging is the Multiquadric Model (Hardy, 1984), a deterministic method, emerging from the discovery of the Multiquadric equation, related to the minimization of the energy integral, and thus relevant to prediction and interpolation applications. The Multiquadric concept was developed from the visualization that a complete multifunction representing irregular surfaces could consist of a linear combination of n single functions (surfaces), with each being centered at a nodal point, which may coincide sequentially with the data points. This method was proven to provide as accurate results as kriging for gravity anomaly prediction, but it offers several advantages in terms of simplicity of formulation as compared to kriging, and numerical efficiency that are particularly important to real-time applications (Wolf, 1981). It should be noted that the MQ method does not provide an accuracy estimate except for the comparison to the data points.

3 Numerical tests

For the numerical analysis, the GPS observations from five stations, with the average separation of ~100km, located in the southern part of the Ohio CORS, were selected (Fig. 2). The Ohio CORS stations are equipped with high-quality GPS receivers, Trimble 5700, connected to choke-ring antennas (http://www.dot.state.oh.us/aerial/Cors.asp). The GPS receivers collect the data with a 1-second sampling rate, while the 60-second sampling rate was selected for the data processing discussed here. Only observations above 20º over the horizon were taken into account.

The data from the magnetically active day of April 29, 2003 (Fig. 3) were processed and analysed. Fig. 3 indicates that the active geomagnetic period started around 12:00 UT, and the Kp index reached the value of six between 18:00-21:00 UT, which reflects a minor geomagnetic storm. The vertical TEC values for this period were obtained according to the methodology presented in the previous section.

The TEC values and the respective IPP coordinates were calculated and saved in two different reference systems:

- geographic (latitude and longitude),
- sun-fixed (geomagnetic latitude and local time).

A geographic reference frame was used to produce the epoch-specific instantaneous regional maps of the ionosphere (e.g., Fig. 6). The sun-fixed reference frame allows creating a "frozen ionosphere" model, referred to the specific time intervals. The "frozen ionosphere" model allows presenting the state of the ionosphere over the region for a 24-hour period in one map (e.g., Fig. 8).

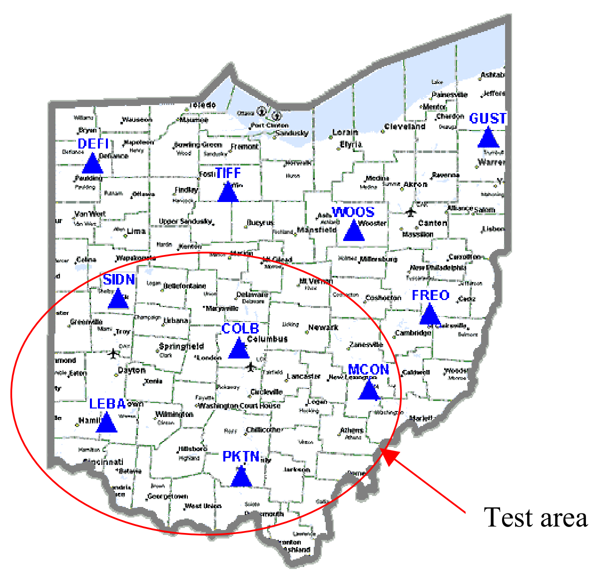

Fig. 2 Map of the Ohio CORS (courtesy of ODOT)

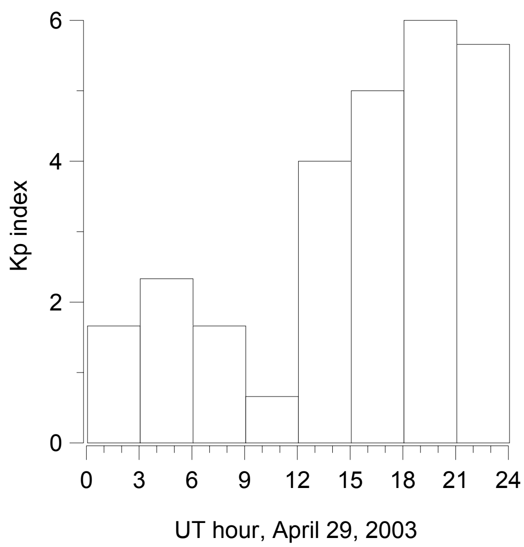

Fig. 3 The values of Kp index during the experiment

After analyzing the geographic location of IPPs for all the observational epochs, a region located between 35º-45º north geographic latitude and 272º-282º longitude was selected to produce the regional ionosphere maps (Fig. 4). This area was covered by IPPs for most of the processed epochs, thus instantaneous ionosphere mapping was ensured.

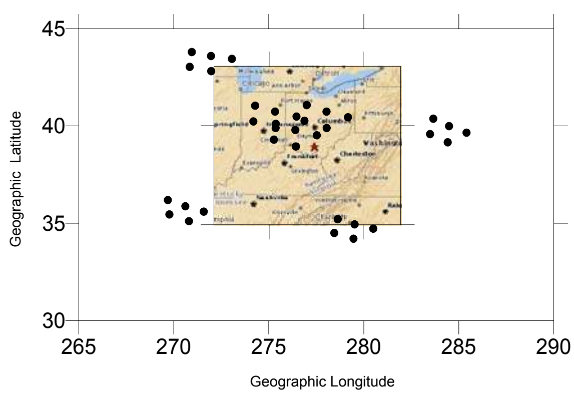

Fig. 4 Example location of IPPs (black dots) at 6:00 UT, April 29, 2003, when seven satellites were simultaneously observed. The background is the area covered by the regional ionosphere model

The TEC values obtained at IPPs were interpolated using kriging and the Multiquadric Model in order to create high-resolution instantaneous regional maps of the ionosphere. The results, produced using the above methods, are compared and analyzed in the following section. In addition, the results from both methods were compared to the reference IGS maps.

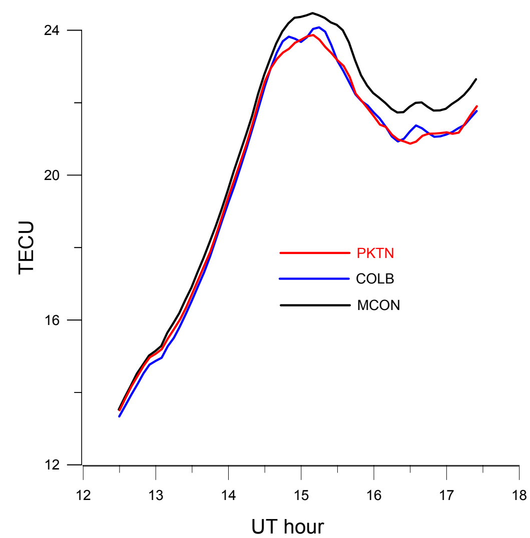

Fig. 5 Comparison of TEC observed to satellite PRN 04 from three CORS stations (COLB, PKTN and MCON) on April 29, 2003

4 Results and analysis

The first analysis presented here is concerned with the internal consistency of the model and the satellite/receiver DCB validation. The TEC values calculated from several CORS stations and GPS satellites were compared. The example presented in Fig. 5 shows that the TEC derived from the observations to PRN 04 is consistent between the neighboring stations, which confirms that the calibrated receiver DCBs are correct. The stations COLB and MCON show exceptionally good agreement.

Fig. 6, left column, presents examples of regional instantaneous ionosphere maps produced using the KR interpolation method. While creating each map, a semi-variogram was calculated and introduced during the data interpolation. The applied approach enables creating the regional ionosphere maps for every observational epoch. Fig. 6 shows the ionosphere maps at the selected epochs. One should keep in mind that the local time for this region is –5 UT hours. The maximum electron density over the investigated area occurred in the local evening, due to, we believe, existing geomagnetic disturbances. The resulting maps may allow detecting the local ionospheric phenomena, e.g., local TEC peaks of 1-3 TECU (Fig. 6). The obtained ionosphere grid has the resolution of 0.08º in latitude and 0.12º in longitude. Such a dense TEC grid can be easily interpolated using simple linear interpolation and used to support satellite navigation.

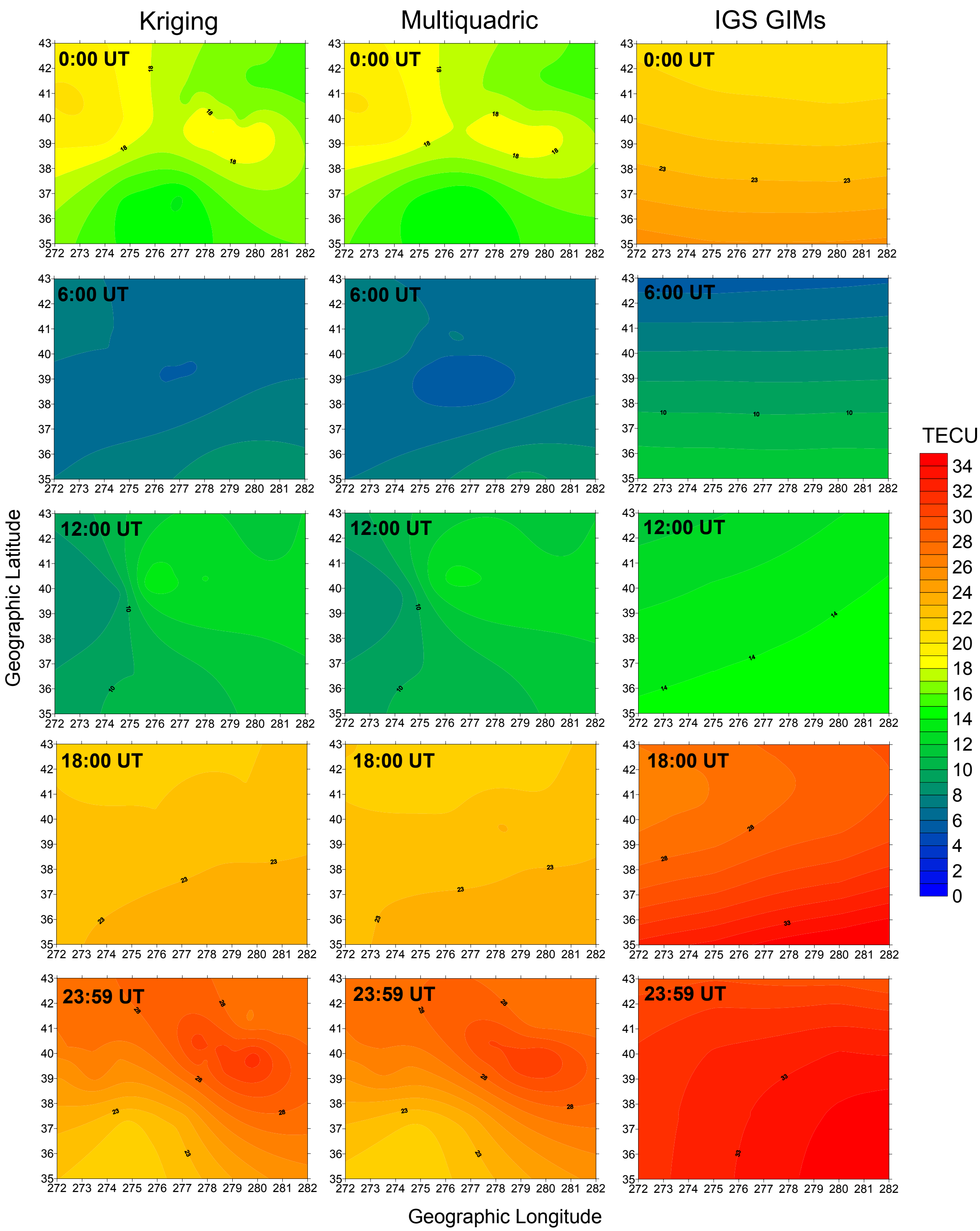

Fig. 6 Comparison between the ionosphere maps for April 29, 2003 derived using KR, MQ and IGS GIMs

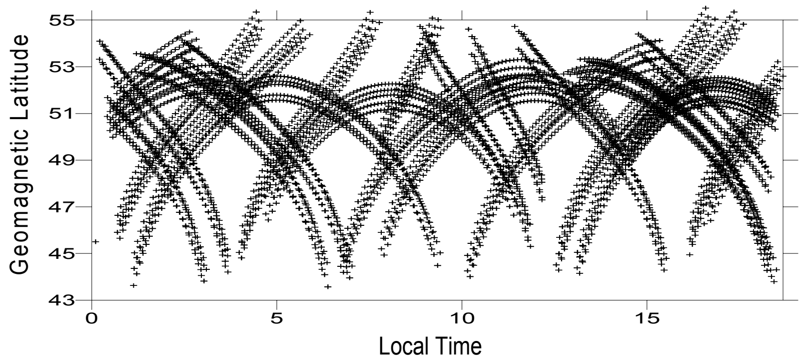

Fig. 7 IPP locations in geomagnetic latitude and local time

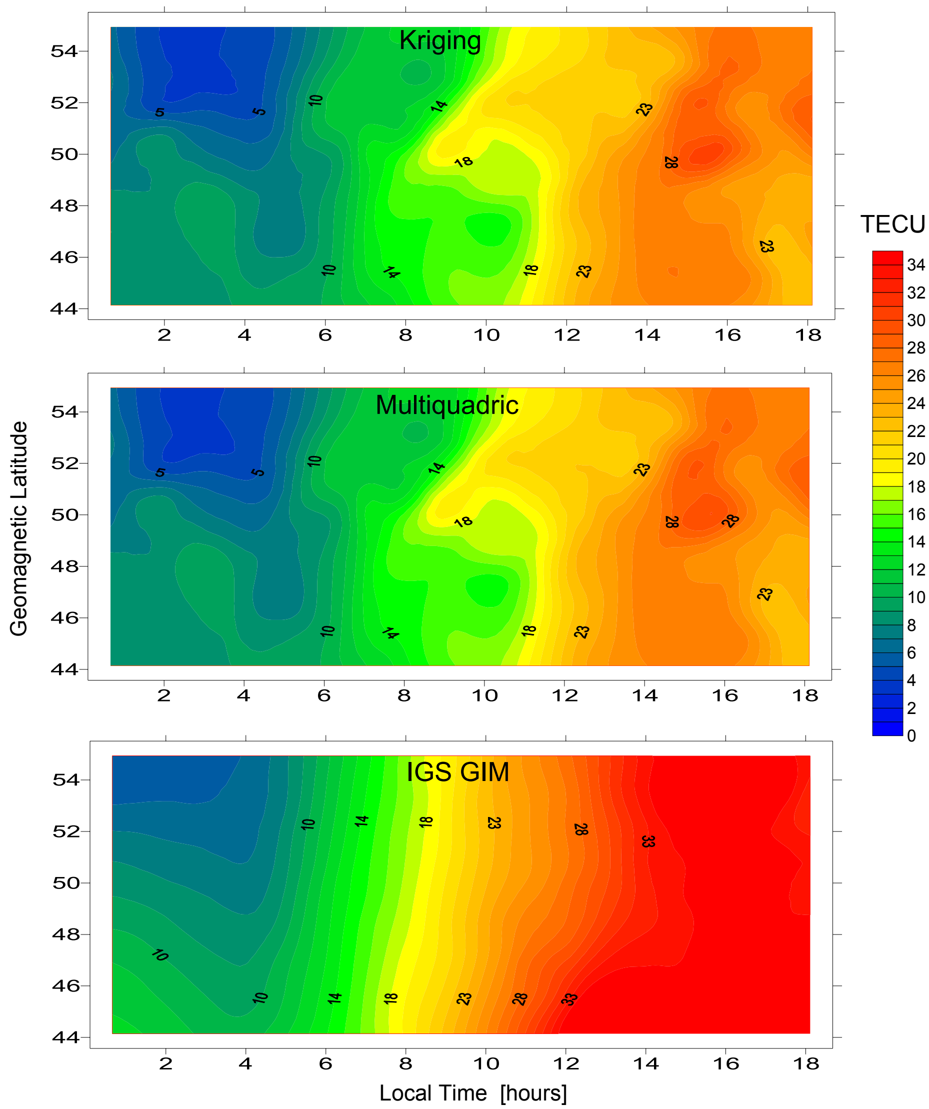

Fig. 8 Regional ionosphere maps for April 29, 2003 in sun-fixed reference frame, derived using KR, MQ and IGS GIMs

Fig. 6, middle column, presents the ionosphere maps generated using the MQ model. The comparison between the results obtained using the KR and MQ methods shows good agreement (similar results were obtained by, for example, Wolf (1981)). The differences in the TEC levels shown by both maps do not exceed 1 TECU. The maps obtained using MQ seems to be a bit smoother, as compared to KR. Owing to the fact that the MQ model is simpler and requires less computational time (in comparison to KR), this method seems to be very promising, especially for real-time applications.

5 Comparison to IGS GIMs

In order to validate the instantaneous regional ionosphere maps, the comparison to IGS GIMs was performed. It should be noted that the IGS GIMs are a combination of GIMs provided by several analysis centers (ACs). All the ACs involved may use different approaches to the TEC derivation from GPS observations, as well as different TEC representation/modeling techniques. As mentioned in the introduction, the spatial resolution of the final IGS GIMs is 2.5º in latitude and 5.0º in longitude.

For comparison purposes, an area covering the regional model was extracted from the IGS GIMs. Fig. 6, right column, presents the example ionosphere maps for the selected epochs extracted from the IGS GIMs. In general, the obtained results are comparable to the IGS GIMs. However, it is noticeable that GIMs general TEC level is higher by about 3-5 TECU, as compared to the maps generated using the KR and MQ methods. This could be explained by the global nature of GIMs. IGS ACs often use TEC representation algorithms, which result in a model resolution comparable with the whole area of the region under investigation (Schaer, 1999). In addition, the sampling rate of the data sets and the network density used in the global and some regional models is much lower than the Ohio CORS investigated here. One should note that the whole investigated region is covered by only 8 GIM grid points. This also explains why the TEC derived from GIMs is very smooth over the region. In contrast to the GIMs, one can observe local features in the ionosphere represented by the regional models. However, some of these features might be caused by a clustered distribution of IPPs (see Fig. 4). Local distribution within the clusters, however, is more than sufficient.

The locations of IPPs in a sun-fixed reference frame are shown in Fig. 7. Their distribution shows that there are still areas with little or no data. Future studies will include the introduction of GPS data from all Ohio CORS stations that should readily improve the IPP coverage and the quality of the regional maps. Fig. 8 illustrates a regional model of the “frozen” ionosphere in geomagnetic latitude and local time coordinate system (sun-fixed). The ionosphere was modeled for the period of 18 hours (5:00 to 23:00 UT or 0:00 to 18:00 LT). Once again, both KR and MQ represent a lower TEC level, as compared to GIM, and show the presence of some local features. Moreover, the ionosphere maps obtained using KR and MQ methods present good agreement. The maximum TEC was observed around 16:00 LT, in contrast to its regular occurrence that usually takes place about 13:00 – 14:00 LT. This might be explained by active geomagnetic conditions (see Fig. 3).

The average TEC level obtained from the CORS GPS data reached 16.94 TECU, and the average TEC level presented by IGS GIMs equals 21.94 TECU (Tab. 1). The minimum and maximum observed TEC is also higher in the case of GIMs (by 2.3 and 4.4 TECU respectively). This significant difference requires more investigation; we speculate that it could occur due to the global nature of GIMs. At the same time, the TEC correlation with the local time is higher for GIMs, which confirms their smooth character that one can observe in Fig. 8. We believe that a regional model should correspond to a more accurate local ionosphere representation. The KR and MQ approaches give a much more detailed picture of the regional ionosphere, since they are able to utilize the information from a dense GPS network. The behavior of the selected ionospheric storms in the regional scale using the proposed models is currently under investigation.

Tab. 1 Statistic of the regional ionosphere

	Regional TEC	IGS GIM
Min. observed TEC level	2.54 TECU	4.82 TECU
Max. observed TEC level	35.24 TECU	39.69 TECU
Average TEC level	16.94 TECU	21.94 TECU
Correlation between TEC and LT	92.9%	97.4%

6 Conclusions and Future Developments

The primary advantages of the instantaneous regional ionosphere mapping presented here are the high temporal and spatial resolutions. The KR and MQ methods applied to the regional GPS data allowed producing more detailed maps of the regional ionosphere, as compared to the global GIMs. In addition, the MQ model needs a very short computational time. It should be mentioned that some of the detected local features could be possibly caused by the relatively small amount of data used here. This phenomenon needs further investigation. Due to the fact that DCBs do not change in the course of a day, their values can be used for several days after the actual calibration. This may allow producing instantaneous TEC maps in near-real time. Since KR and MQ are suitable for extrapolation, they enable forecasting of the ionosphere in order to support radionavigation. Both methods seem to be suitable for instantaneous regional ionosphere modeling.

The current disadvantage of the presented approach is the use of receiver DCBs produced by external software. Ongoing developments include the receiver DCB estimation module. The IGS-provided satellite DCBs will still be used, as they are routinely available and of high quality. Future studies will include all Ohio CORS stations in an attempt to produce regional maps with a few-minute data accumulation. A final regional ionosphere model for the State of Ohio will be used to support the precise point positioning (PPP) module in Multi-Purpose GPS Processing Software (MPGPS™), which is under development at OSU.

Presented here is only the evaluation of the ionosphere, with no inclusion of the ionospheric information to the positioning results. Therefore, the future study will also cover a comparison of the positioning results using GIMs and the proposed regional solution.

Acknowledgments

This work is supported by NOAA, National Geodetic Survey, NGS (project DG133C-02-SE-0759), and SOI - Survey of Israel (project 2002-11). Dr. Pawel Wielgosz is supported by the Foundation for Polish Science.

References

Blanch J. (2002) ***An Ionospheric Estimation Algorithm for WAAS Based on Kriging***, Proceedings of ION GPS 2002, Portland, OR.

Feltens J. and N. Jakowski (2002) ***The International GPS Service (IGS) Ionosphere Working Activity***, SCAR Report No. 21.

Gao Y. and Z.Z. Liu (2002) ***Precise Ionosphere Modeling Using Regional GPS Network Data***, Journal of Global Positioning Systems, Vol. 1, No. 1, 18-24.

Hardy R.L. (1984) ***Kriging, collocation, and biharmonic models for applications in earth sciences***, Tech. Papers of the American Congress on Surveying and Mapping, pp. 363-372.

Hernandez-Pajares M., J.M. Juan, J. Sanz and O.L. Colombo (1999) ***Precise ionospheric determination and its application to real-time GPS ambiguity resolution***, Proceedings of ION GPS'99, Nashville, TN.

Hugentobler U., S. Schaer and P. Fridez (2001) ***BERNESE GPS Software Version 4.2***, Astronomical Institute, University of Berne, Switzerland.

Komjathy A. (1997) ***Global Ionospheric Total Electron Content Mapping Using the Global Positioning System***, Ph.D. dissertation, Department of Geodesy and Geomatics Engineering Technical Report No. 188, University of New Brunswick, Canada, 248 pp.

Li T.-H. (1999) ***Multiscale Representation and Analysis of Spherical Data by Spherical Wavelets***, SIAM Journal on Scientific Computing, Vol. 21, No. 3, pp. 924-953.

Mannucci A.J., B.D. Wilson and C.D. Edwards (1993) ***A New Method for Monitoring the Earth Ionosphere Total Electron Content Using the GPS Global Network***, Proceedings of ION GPS'93, pp. 1323-1332.

Schaer S. (1999) ***Mapping and Predicting the Earth's Ionosphere Using the Global Positioning System***, Ph.D. Thesis, Astronomical Institute, University of Berne, 205 pp.

Schmidt M. (2001) ***Grundprinzipien der Wavelet-Analyse und Anwendungen in der Geodäsie***. Habilitationsschrift, Shaker Verlag, Aachen.

Springer T.A. (1999) ***Modeling and Validating Orbits and Clocks Using the Global Positioning System***, Ph.D. dissertation, Astronomical Institute, University of Berne, Switzerland, 155 pp.

Stanislawska I. and L.R. Cander **(1999)** ***Coordinated SRC and RAL Centres for ionospheric weather specification and forecasting*****,** ESA Workshop on Space Weather, 11-13 November 1998, ESTEC, Noordwijk, The Netherlands, WPP-155, pp. 499-552.

Stanislawska I., G. Juchnikowski, R. Hanbaba, H.Rothkaehl, G.Sole and Z. Zbyszynski (2000) ***COST 251 Recommended Instantaneous Mapping Model of Ionospheric Characteristics – PLES***, Phys. Chem. Earth (C), vol. 25, no. 4, pp. 291-294.

Stanislawska I., P.A. Bradley and G. Juchnikowski (2002) ***Spatial correlation assessment of ionospheric parameters for limited-area mapping*****,** Proceedings of the XXVIIth General Assembly of the International Union of Radio Science, Maastricht, Netherlands 17-24 August 2002.

Webster R. and M. Olivier (2001) ***Geostatistics for Environmental Scientists***, John Wiley and Sons, New York.

Wielgosz P., L.W. Baran, I.I. Shagimuratov and M.V. Aleshnikova (2003) ***Latitudinal variations of TEC over Europe obtained from GPS observation***, accepted by Annales Geophysicae.

Wolf H. (1981) ***Multiquadratische Methode und Kollokation***, AVN – Aligemeine Vermessung-nachrichten, Marz 1981.